We are IntechOpen, the world's leading publisher of Open Access books Built by scientists, for scientists

6,900
Open access books available

186,000
International authors and editors

200M
Downloads

Our authors are among the

154
Countries delivered to

TOP 1%
most cited scientists

12.2%
Contributors from top 500 universities

WEB OF SCIENCE™

Selection of our books indexed in the Book Citation Index in Web of Science™ Core Collection (BKCI)

Interested in publishing with us?
Contact book.department@intechopen.com

Numbers displayed above are based on latest data collected.
For more information visit www.intechopen.com

12

Synthesis and Thermophysical Characterization of Bismuth based High-T_c Superconductors

M. Anis-ur-Rehman[1] and Asghari Maqsood[2]
[1]*Applied Thermal Physics Laboratory, Department of Physics, COMSATS Institute of Information Technology, Islamabad 44000*
[2]*Thermal Transport Laboratory, SCME, National University of Sciences and Technology (NUST), Islamabad*
Pakistan

1. Introduction

Dissipation phenomena in high temperature superconductors are directed by the microstructure that builds up during the preparation process. Therefore, detailed investigations of the electrical and thermal transport and ac magnetic susceptibilities in superconductors prepared either in the form of single crystals, thin films or polycrystalline are important for understanding superconductivity as well as for useful applications.
The effect of elements (Pb, Fe, Co, Ni, V, Zn) doping in Bi-based superconducting materials has been extensively investigated (Remschnig et al., 1991; Awana et al., 1992; Maeda et al., 1990; vom Hedt et al., 1994; Pop et al., 1997; Mori et al. 1992; Kim et al., 1992; Gul et al., 2008; Maqsood et al., 1992). It was reported that the superconducting properties of these materials are affected with increase of the amount of doping, regardless of the nature of the dopants. The repression of superconductivity was concluded to be due to local disorder induced by the amount of doping. However, the details of the current limiting means in the Bi-2223 system are not well established. Consequently, it is of interest to try these doping elements in the Bi-2223 system with a different nominal composition, of which we intend to investigate $Bi_{1.6}Pb_{0.4}Sr_{1.6}Ba_{0.4}Ca_2Cu_3O_y$ in order to provide additional observations to contribute further understanding of their role on the superconductivity of the system.
It is well established that ceramic high-*T*c superconductors include a collection of tiny, randomly oriented anisotropic grains which are connected to each other by a system of so called 'weak links' or 'matrix'. The linear temperature dependence of the electrical resistivity is one of the most important characteristics of the normal phase kinetics of high-T_c layered cuprates (Batlogg, 1990).
In superconductors where the dc electrical resistivity diverges to zero below T_c, the thermal conduction is almost a unique measurement to study the transport properties below T_c. The magnitude and temperature dependence of the thermal conductivity are parameters which have an impact on a broad spectrum of devices. In high-T_C superconductors, such information is even more valuable to know how the free carriers and lattice vibrations contribute to the transport of heat. Transient Plane Source (TPS) technique is a well

developed and a well known method (Gustafsson, 1991; Maqsood, 1994; Maqsood, 1996) to study the thermal transport properties. For TPS method a single transition phase will be of great help to study such properties. Multiple phases, in the material, will make the situation more complicated and an increase in measurement errors also. The TPS technique is modified and improved for the measurements of thermal transport properties of high-T_c superconductors. The modified arrangement is referred to as the Advantageous Transient Plane Source (ATPS) technique (Rehman, 2002). The circuit components are reduced with this new arrangement as compared to the bridge used earlier (Maqsood, 2000). The modified bridge arrangement is already calibrated with fused quartz, carbon steel and AgCl crystals (Rehman, 2002; Rehman, 2003).

Peltier refrigerators use the thermoelectric materials for refrigeration. Peltier thermoelectrics are more reliable than compressor based refrigerators, and are used in situations where reliability is critical like deep space probes. Thermoelectric material applications include refrigeration or electrical power generation. Thermoelectric materials used in the present refrigeration or power generation devices are heavily doped semiconductors. The metals are poor thermoelectric materials with low Seebeck coefficient and large electronic contribution to the thermal conductivity. Insulators have a large Seebeck coefficient and a small contribution to the thermal conductivity, but have too few carriers, which result in a large electrical resistivity. The Figure of merit is the deciding factor for the quality of thermoelectric materials. In order to increase the whole Figure of merit, it is of interest to replace the p-type leg of the Peltier junction by a thermoelectrically passive material with a Figure of merit close to zero (Fee, 1993). This is why it is interesting to study the Figure of merit of the ceramic superconductors.

One of the important thermomagnetic transport quantities is the electrothermal conductivity and is shown to be one of the powerful probes of high-temperature superconductors. Cryogenic bolometers are sensitive detectors of infrared and millimeter wave radiation and are widely used in laboratory experiments as well as ground-based, airborne, and space-based astronomical observations (Richards, 1994). In many applications, bolometer performance is limited by a trade off between speed and sensitivity. Superconducting transition-edge bolometer can give a large increase in speed and a significant increase in sensitivity over technologies now in use. This combination of speed with sensitivity should open new applications for superconducting bolometric detectors (Leea et al., 1996).

Other potent applications for electrothermal conductivity of superconductors is actuators in MEMS technologies, electrothermal rockets etc (Microsoft Encarta Encyclopedia, 2003).

The temperature dependence of the dc electrical resistivity, along with low field ac magnetic susceptibility, X-ray diffraction, thermal transport, electrothermal conductivity and thermoelectric power studies and calculations of Figure of merit factor are reported here.

2. Experimental

2.1 Preparation and characterization

In the Bi-based high-T_c superconductors the Bi-2223 phase is stable within a narrow temperature range and exhibits phase equilibrium with only a few of the compounds existing in the system (Majewski, 2000). Precise control over the processing parameters is required to obtain the phase-pure material (Balachandran et al., 1996). All samples were prepared from 99.9% pure powders of Bi_2O_3, PbO, $SrCO_3$, $BaCO_3$, $CaCO_3$ and CuO. The powders were mixed to give nominal composition of $Bi_{1.6}Pb_{0.4}Sr_{1.6}Ba_{0.4}Ca_2Cu_3O_y$ and were thoroughly ground in an

agate mortar to give very fine powder. The grind powder was calcined for 21 hours in air at 800°C. A series of pellets was produced in two sizes, from this well mixed material and controlled heating and cooling carried out, in air, using a horizontal tube furnace. Poly Vinyl Alcohol (PVA) was used as binder in the samples. PVA is one of the few high molecular weight polymers, which is water soluble and is dry solid, commercially available in granular or powder form. The properties of Poly Vinyl Alcohol vary according to the molecular weight of the parent poly vinyl acetate and the degree of hydrolysis. Fully hydrolyzed form with medium viscosity grade PVA was used in our case. Samples were in the shape of cylindrical disks having diameters 13mm and 28mm, and lengths 3mm and 11mm respectively. These samples were sintered at 830°C for the intervals of 24 hours in each sintering step as sintering procedures do affect the properties (Rehman et al., 1998).

The superconducting properties were characterized electrically by using standard four probe method. Contacts were made by high quality silver paste. The temperature was measured by using a calibrated Pt-100 thermometer.

Low field ac susceptibility measurements are very important for the characterization of high-temperature superconductors (Chen et al., 1989; Muller, 1989; Ishida & Goldfarb, 1990; Celebi, 1999). The sharp decrease in the real part χ' (T) below the critical temperature T_c is a manifestation of diamagnetic shielding. Ac susceptibility of the sample was measured after each sintering step. The low field ac susceptibility properties were studied by the use of mutual inductance bridge method. The measurements were taken from room temperature down to 80K.

X-ray diffractograph (XRD) of sample was taken after the final sintering. The radiation used for XRD was CuK_α and the measurements were made at room temperature. Measurements were done at room temperature since there is no change in the structure of the superconducting materials before and after transition (Rehman et al., 1998; Jasiolek et al. 1990).

2.2 Thermal transport properties

Thermal transport measurements, i.e. thermal conductivity, thermal diffusivity and heat capacity per unit volume were performed using the Advantageous Transient Plane Source (ATPS) Technique (Rehman & Maqsood, 2002; Rehman & Maqsood, 2003). Circuit diagram for the method is shown in Fig. 1. Simultaneous measurement of thermal conductivity and thermal diffusivity is the foremost advantage of this technique. Heat capacity per unit volume is then calculated using the idea that, if all heat is transported via solid specimen then the thermal conductivity (λ), thermal diffusivity (κ) and heat capacity per unit volume (ρC_p) are expressed by;

$$\kappa = \frac{\lambda}{\rho C_p} \tag{1}$$

A detailed description of this experimental technique can be found elsewhere (Gustafsson, 1991). The ideal model presupposes that the double spiral sensor, assumed to consist of a set of equally spaced, concentric, and circular line heat sources, is sandwiched in specimens of infinite dimensions. In practice all real specimens do have finite dimensions. However, by restricting the time of the transient, which relates to the thermal penetration depth of the transient heating, a measurement can still be analyzed as if it was performed in an infinite medium. This means that the ideal theoretical model is still valid within a properly selected

time window for the evaluation. The scatter in thermal conductivity measurements is about 0.14% and is 0.66% and 0.52% in thermal diffusivity and volumetric heat capacity respectively (Rehman & Maqsood, 2002; Rehman & Maqsood, 2003). Taking into consideration the limitations of the theory of the technique and the experimental sampling errors, the thermal conductivity and thermal diffusivity data contain errors of 4% and 7% respectively. The errors in volumetric heat capacity are around 10% (Rehman & Maqsood, 2002; Maqsood et al., 2000; Rehman & Maqsood, 2003).

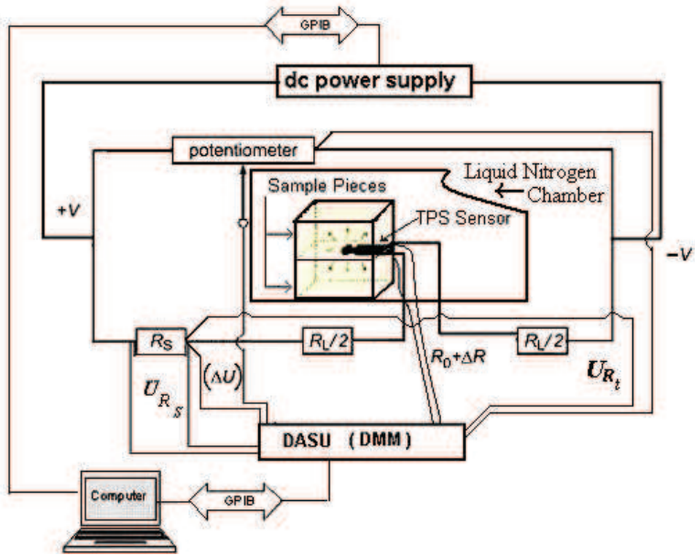

Fig. 1. Circuit diagram for the Advantageous Transient Plane Source (ATPS) technique

2.3 Thermoelectric power measurements

An easy to use and simple apparatus was designed and developed for thermoelectric power (S) measurements. Circuit diagram along with the sample holder assembly is shown in Fig. 2. The sample is subjected to a temperature difference ΔT using a heating resistor and corresponding voltage difference ΔV across the sample is measured. Thermoelectric power is obtained by taking ratio of the voltage difference to the temperature difference. Chromel-alumel thermocouples are used for measuring the temperature difference, ΔT. The thermocouples are electrically isolated from the sample and thermally connected to the sample. Heat losses through the electrical connections are minimized using long leads wrapped around a Teflon tube. The voltage leads are then silver pasted to the sample in the vicinity of thermocouples to assure that the voltage and temperature gradients are measured at the same locations on the sample for accurate thermoelectric power measurements. The next step includes loading the sample assembly into the sample chamber and evacuation of the chamber. The chamber is evacuated to eliminate any water vapour condensation on the sample, which can result in erroneous measurements. Dry nitrogen gas is then filled in the chamber as a conducting media between chamber walls and the sample. This sample chamber is then inserted in liquid nitrogen container for cooling. Data are collected under the computer control. By incorporating multiple measurements in a single run, considerable time is saved by avoiding remounting, and recooling of the samples. In this technique the surface mount resistor (50Ω) was used to heat one end of the sample to establish a measured temperature gradient of approximately 1K.

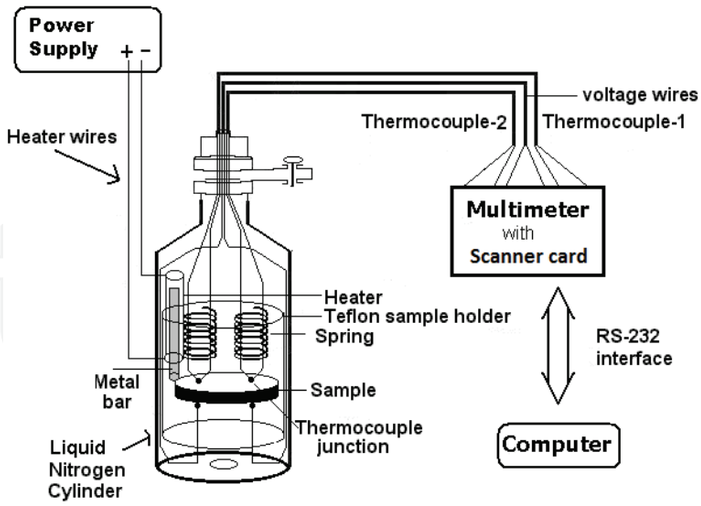

Fig. 2. Block diagram of the apparatus developed for thermoelectric power measurements. Scanner card is used with the multimeter for simultaneous measurements at different points as shown. RS-232 is the standard serial interface of the computer

3. Experimental results and discussion

3.1 Dc electrical resistivity

Variation of resistivity with change in temperature is recorded for after each sintering step and the plots are given in Fig. 3.

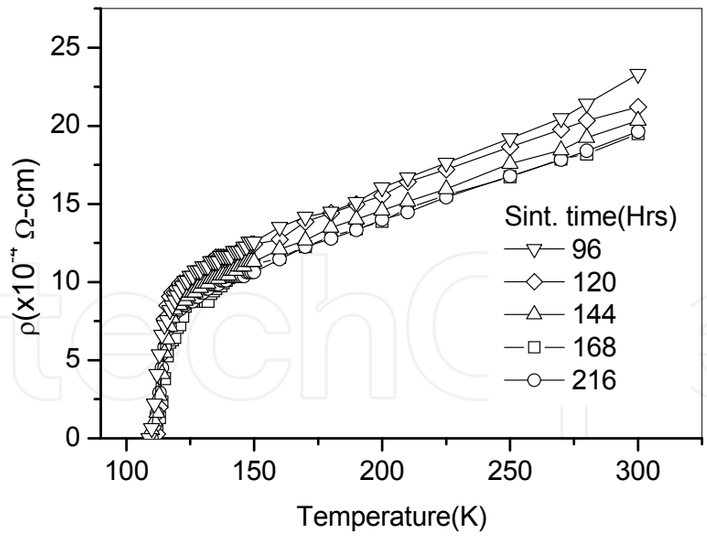

Fig. 3. DC electrical resistivity as a function of temperature for the sample after each sintering step

One of the most striking features about the cuprate superconductors is the behavior of the resistivity of the normal state that is found above the transition temperature of the optimally doped materials. After the final sintering the measured density of the sample was 3.48 gcm^{-3} and $T_{c,0}$ was 110 ± 1K. The added barium (Ba) has increased the $T_{c,0}$. Residual resistivity was

0.19 mΩ-cm and the intrinsic resistivity was 5.9 μΩ-cmK^{-1}. The ratio ρ(273K)/ρ(4.2K) is the residual resistivity ratio (RRR), an important parameter in the design of superconductive applications. In the case of a superconductor, the denominator has to be taken at a temperature slightly above the critical temperature (Seeber, 1998). RRR in our case was in the range 23-33.

3.2 Ac susceptibility

Ac susceptibility measurements were done after each sintering step (Fig. 4).

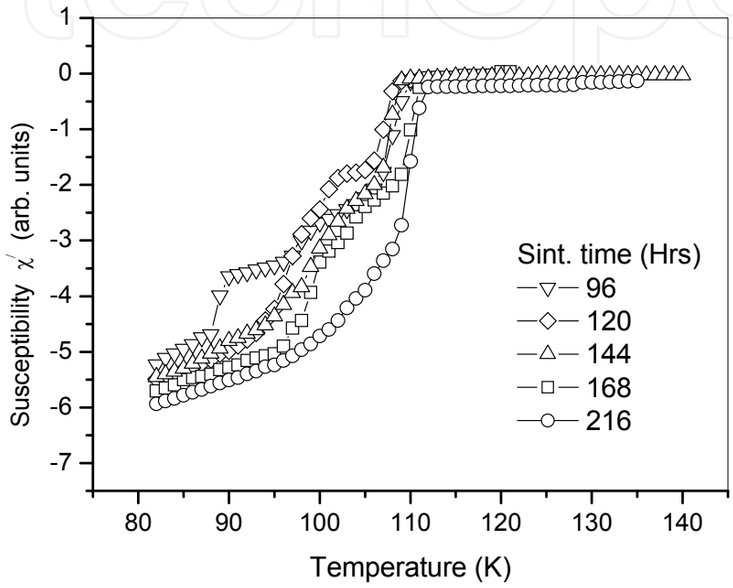

Fig. 4. Variation of ac susceptibility (real part), with temperature after each sintering step

Initially two transition phases were present. One of the identified phases is the Bi-2212(low T_c) phase and the other Bi-2223(high T_c) phase. With sintering, the low T_c phase was smoothed out and only phase left is the Bi-2223(high-T_c) phase. Although the resistivity variation with temperature was smoothed out after the third sintering but slight kinks were observed in the susceptibility against temperature plot showing the more sensitivity of the measuring method.

3.3 X-ray diffraction studies

Almost all the peaks are indexed. The only phase is the orthorhombic high-T_c Bi-2223 phase. Lattice parameters were calculated from the (h k l) values of the indexed peaks. The lattice parameters are a = 5.42 (1) Å, b = 5.37 (1) Å and c = 37.12 (8) Å. No peaks were found matching the Bi-2212 low T_c phase. Indexed X-ray diffractograph is shown in Fig. 5.

The lattice constants agreed with the previous reports (Maqsood et al., 1996). The size of the grains in polycrystalline materials has pronounced effects on many of its properties. Using Scherrer's equation [29];

$$B = \frac{0.9\lambda}{t\cos\theta} \tag{2}$$

where;
B = Broadening of diffraction line measured at half its maximum intensity (radians), λ = Radiation source wavelength and t = Diameter of crystal particle,
particle sizes are determined and the diameter of the crystal particles lies between 172 – 512 Å.

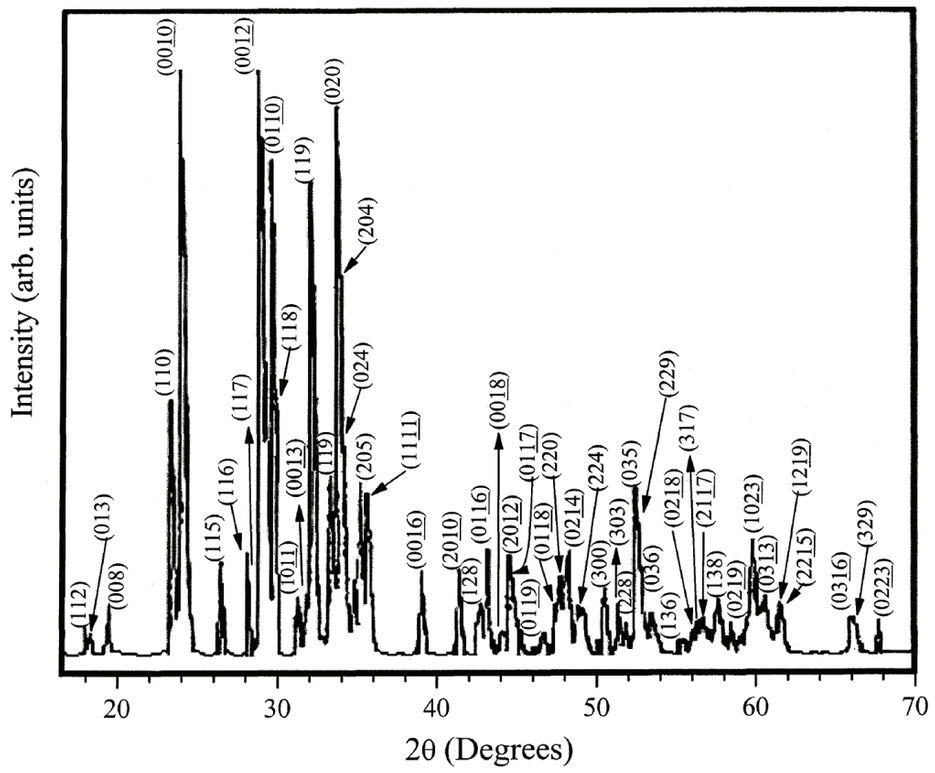

Fig. 5. Indexed x-ray diffraction pattern of the sample after the final sintering at room temperature

3.4 Thermal properties measurements

After the preliminary characterization of the samples and existence of almost a single phase, large disc-shaped samples (28 mm diameter and 11 mm thickness) were used for the thermal measurements. Fig. 6 shows the temperature dependence of the thermal conductivity λ. As the temperature decreases, the conductivity gradually decreases down to near T_c then remarkably increases below T_c. Further decrease in temperature was not possible, due to limitation of the cryostat used, to take the maximum in λ. This temperature dependence agrees with the widely observed behavior of λ for the oxide superconductors (Uher & Kaiser, 1987; Peacor & Uher, 1989; Mori et al., 1989; Crommie & Zettle, 1990; Cohn et al., 1992).
Comparing the results between different laboratories, one notes that the thermal conductivity depends on a particular sample preparation process. The temperature dependence of the conductivity is really similar for all the samples (Ginsberg, 1992; Ikebe et al. 1994) . So the order of magnitude of thermal conductivity (measured by non-steady state

method in our case) is comparable to the results obtained by different authors (measured by steady state methods).

Fig. 6 also shows the variation of measured thermal diffusivity κ with temperature for the sample. Between 294K and T_c, κ increases very gradually with decreasing temperature. The increase of κ becomes very large around T_c and become very steep.

The heat capacity per unit volume, ρC_p, calculated from the thermal conductivity measurements and thermal diffusivity measurements using equation 1 is shown in Fig. 6. ρC_p decreases with decrease in temperature and near T_c a sizeable kink is observed. This jump is mostly due to the improved sharpness of the transition related to the reduction of

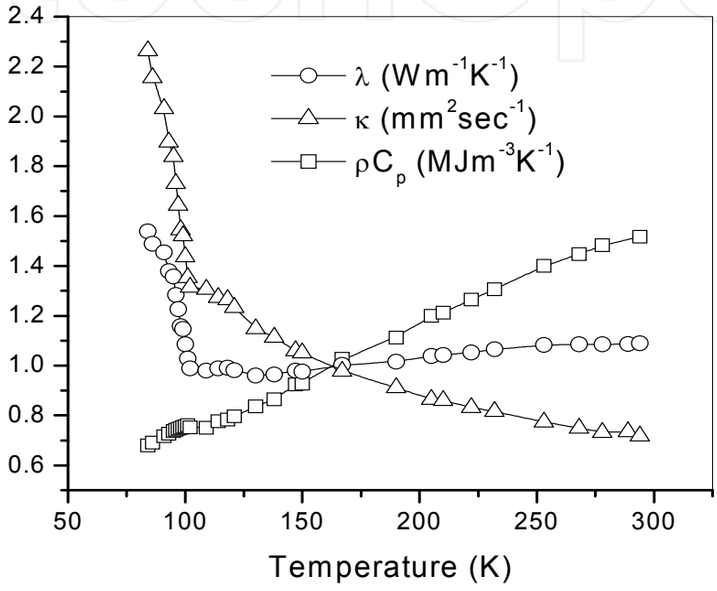

Fig. 6. Variation in thermal transport properties with temperature for the sample $^{Bi}1.6^{Pb}0.4^{Sr}1.6^{Ba}0.4^{Ca}2^{Cu}3^{O}y$

intergrowth structure by adding Pb (Okazaki et al., 1990) and is improved by adding Ba in our case. Since the calculated lattice constants of our sample are similar to Bi-2223 composition so it is assumed that oxygen is 10, and then the composition becomes $Bi_{1.6}Pb_{0.4}Sr_{1.6}Ba_{0.4}Ca_2Cu_3O_{10}$. Also there is no change in the density of the superconducting sample in the studied temperature range so the value of specific heat C_p is calculated. The absolute value of C_p is 320 $Jmol^{-1}K^{-1}$ at 180K and that is similar to already reported value of a similar composition (Okazaki et al. 1990; Gordon et al. 1991). Because the phonon contribution is by far dominant than the electronic contribution in the temperature range studied, the specific heat data fitted to the following Debye formula,

$$C_{p-ph} = 9nR\frac{T^3}{\Theta_D^3}\int_0^{\Theta_D/T}\frac{x^4 e^x}{(e^x-1)^2}dx \tag{3}$$

where $C_{p\text{-}ph}$ is molar specific heat, x is the reduced phonon frequency, n (= 19) the number of atoms composing Bi(Ba) 2223 molecules, R the gas constant and Θ_D is the Debye temperature. Although a single Θ_D fitting fails to give a unified strict fitting over the entire temperature range, but Θ_D = 510 K gives a satisfactory fitting between T = 120 to 230 K as is shown in Fig. 7.

3.5 Thermoelectric power

To check the calibration of this new apparatus (Fig. 2), thermoelectric power of copper was measured in the temperature range 85-310K. Results of our measurements are shown in Fig. 8 indicating an agreement with the already published data (Barnard, 1972).

The standard deviation in the data was between 0.01-0.22 μVK^{-1} and the difference between measurements done in this work and the already published (Barnard, 1972) data were within 5%.

The thermoelectric power of the high-T_C superconducting sample was measured in temperature range 85-300K. The thermoelectric power (S) reached zero within experimental uncertainty in superconducting state. The thermoelectric power increased with decrease in temperature and after reaching T_c value, thermoelectric power decreased strongly to zero value (Fig. 9).

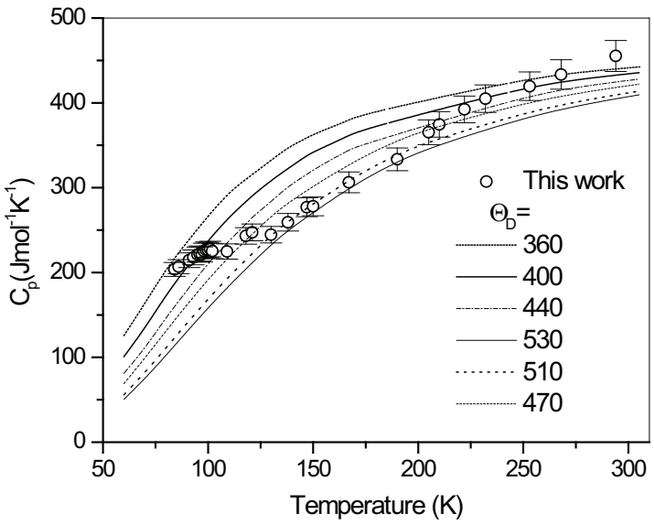

Fig. 7. The specific heat estimated from thermal conductivity (λ) and thermal diffusivity (κ). Calculated values for different values of Θ_D are also shown.

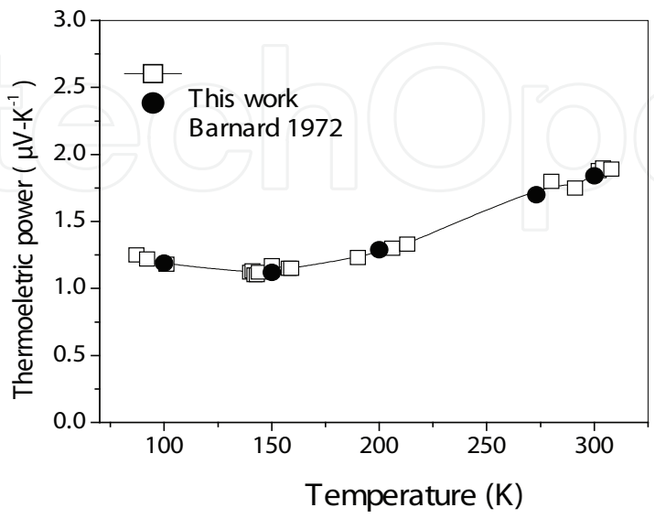

Fig. 8. Thermoelectric power of the copper sample with temperature.

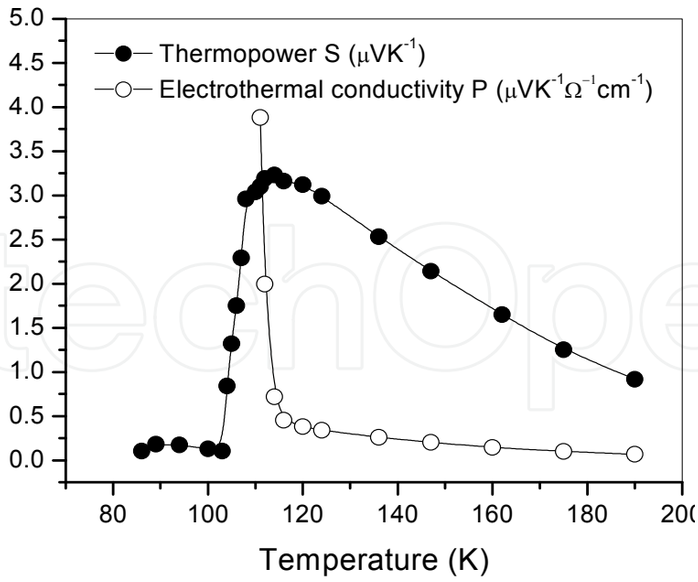

Fig. 9. Variation of thermoelectrical power (S) and electrothermal connductivity (P) with temperature for the sample

At high temperatures the thermoelectric power is almost linear. Thus we can use the Mott expression to determine the Fermi level (Barnard, 1972; Bougrine et al., 1998):

$$S = S_0 - \frac{\pi^2 k_B{}^2}{3|e|E_F} T \tag{4}$$

where S_0 is a constant. From the slope (-0.03145 μV / K²) estimated by a linear extrapolation we have found the Fermi level to be 0.78 eV.

Similar profile for the same kind of superconductors is reported (Mitra et al., 1998; Chen et al., 1989; Laurent et al., 1989; Lopez et al., 1991; Naqvi et al., 1997; Pekala et al. 1996).

3.6 Electrothermal conductivity

The electrothermal conductivity (P) is the thermoelectric power divided by the dc electrical resistivity and is given as,

$$P = \frac{S}{\rho} \tag{5}$$

Where S is the thermoelectric power and ρ is the dc electrical resistivity.

In the mixed state of a superconductor, the electrothermal conductivity is also defined as the measure of the electrical current density produced by a thermal gradient and is supposed to be independent of the magnetic field. We have utilized the former definition to calculate electrothermal conductivity as shown in Fig. 9.

3.7 Figure of merit

Using the data of electrical resistivity, thermal conductivity and thermoelectric power, Figure of merit factor is calculated and is plotted in Fig. 10.

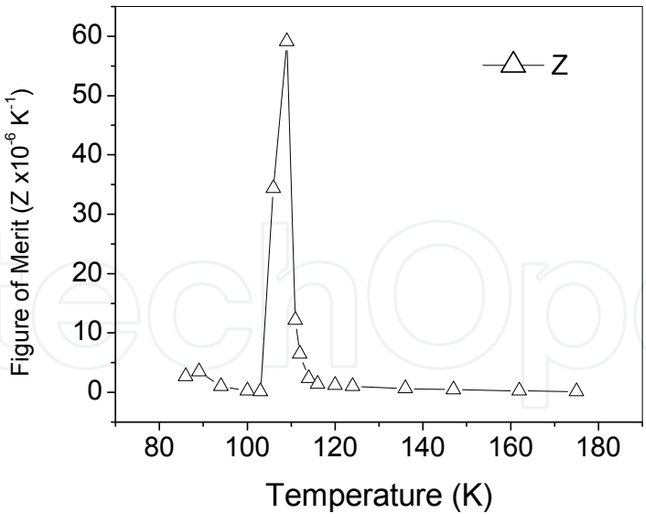

Fig. 10. Variation of Figure of Merit Factor (Z), with temperature.

The Figure of merit is calculated from the expression (Bougrine et al., 1998),

$$Z(T) = \frac{S^2(T)}{\lambda(T)\rho(T)} \tag{6}$$

Where: Z(T) is the Figure of merit factor, S(T) is the thermoelectric power, λ(T) is the thermal conductivity and ρ(T) is the electrical resistivity.

Near critical temperature the Figure of merit present a remarkable peak for the samples. This peak is due to a quick drop in the electrical resistivity which occurs about 3K before the drop in thermoelectric power. Outside the critical temperature region one can see that the curves of the Figure of merit and thermoelectric power are characterized by a similar behaviour near T_c. Similar trend of the Figure of merit is observed in the Bi-based high-T_c superconductors (Bougrine et al., 1998).

4. Summary and conclusions

The samples with nominal composition $Bi_{1.6}Pb_{0.4}Sr_{1.6}Ba_{0.4}Ca_2Cu_3O_Y$ were synthesized by a solid state reaction method with controlled synthesis process to get the preferred single phase. This composition was chosen on the basis of experiments conducted by the authors with a similar composition (Maqsood et al., 1992). The samples were almost a single phase with Bi-2223 high-T_c phase recognized. All the three types of tests i.e. dc electrical resistivity, ac magnetic susceptibility and x-ray diffraction are in conformity with each other, all validating almost a single Bi-2223 high-T_c phase. Single transition phase in the material and fabrication of homogenous samples in large sizes favored the Advantageous Transient Plane Source (ATPS) technique for thermal transport measurements. Thermal transport properties include thermal conductivity, thermal diffusivity and heat capacity per unit volume. Synchronized measurement of thermal conductivity and thermal diffusivity makes it possible to estimate specific heat and the Debye temperature Θ_D. The simultaneous measurement also provides a useful check on the consistency and the reliability of the analyses. Thermal conductivity variation with temperature shows slight decrease initially

and then a pronounced increase around T_c. A similar behaviour is observed in all hole-type CuO_2-plane superconductors and in all their structural forms. This effect is due to phonon (Tewordt & Wolkhausen, 1988) or quasiparticle scattering (Houssa and Ausloos, 1994). Thermal diffusivity shows a similar tendency as that of the thermal conductivity. Heat capacity per unit volume decreases with decrease in temperature. Assuming density of the sample to be constant in the studied temperature range molar specific heat is also calculated. Specific heat jump around T_c is also very prominent. These results indicate a good crystalline structure and the most favorable doping. Thermoelectric power was positive in the studied bismuth-based superconductor. The behavior of thermoelectric power of the sample was approximately linear with temperature as observed in other bismuth-based high-T_C superconductors. The superconducting transition started at 114±1K and after that, thermoelectric power reduced almost to zero value at 103±1K. The known value of the transition temperature of this sample measured from electrical resistivity was 110±1K. Therefore, the difference between thermoelectric transition temperature and resistivity transition temperature were almost in agreement within experimental errors. Electrothermal conductivity increases sharply near the transition temperature. A maximum in the Figure of merit, of this ceramic superconductor, is around the superconducting transition temperature. It is then reduced to zero below critical temperature. This system can be valuable for application in low-temperature Peltier devices in order to reach temperatures lesser than the temperature of liquid nitrogen.

5. References

Awana V.P.S., Agarwal S.K., Kumaraswany B.V., Singh B.P., Narlikar A.V. (1992). *Supercond. Sci. Technol.* 5 376.

Balachandran U., Iyer A.N., Haldar P., Hoehn J.G., Motowidlo L.R., H Maeda, Togano K. (1996). (Eds.), *Bi-Based High-T_c Superconductors*, Marcel Decker Inc., New York

Barnard R.D. (1972) *Thermoelectricity in metals and alloys*, Taylor & Francis Ltd., London,

Batlogg B. (1990). *High temperature superconductivity*, Addison-Wesley, Redwood city, CA

Bougrine H., Ausloos M., Cloots R., Pekala M. (1998) Proc. 17th International conference on thermoelectrics, IEEE

Celebi S. (1999). *Physica C* 316 251

Chen G.H., Yang G., Yan Y.F., Jia S.L., Ni Y.M., Zheng D.N., Yang Q.S., Zhou Z.X. (1989). *Mod. Phy. Lett. B* 3 1045

Chen D.X., Nogues J., Rao K.V.(1989). *Cryogenics* 29 800

Cohn J.L., Wolf S.A., Vanderah T.A. (1992). *Phys. Rev. B* 45 511.

Crommie M.F., Zettle A. (1990). *Phys. Rev. B* 41 10978.

Cullity B.D. (1967). *Elements of X-ray diffraction* 3rd ed., Addison-Wesley Publishing Company, Inc., London

Fee M. (1993). *Appl. Phys. Lett.* 62 1161

Ginsberg D.M. (1992). *High Temperature Superconductivity*, World Scientific Publishing Co. Pte. Ltd.

Gordon J.E., Prigge S., Collocott S.J. , Driver R. (1991). *Physica C* 185-189 1351

Gul I.H., Maqsood A. (2008). *J. Supercond. Nov. Magn.* 399-407 21.
Gustafsson S.E. (1991). *Rev. Sci. Instrum.* 62 797
Houssa M., Ausloos M. (1994). *Physica C* 235 1483
Ikebe M., Fujishiro H., Naito T., Noto K. (1994). *J. Phys. Soc. Japan.* 63 3107
Ishida T., Goldfarb R.B. (1990). *Phys. Rev. B* 41 8937
Jasiolek G., Gorecka J., Majewski J., Yuan S., Jin S., Liang R. (1990). *Supercond. Sci. Technol*. 3 194
Kim S.H., Kim H.S., Lee S.H., Kim K.H. (1992). *Solid State Commun.* 83 127
Laurent C., Patapi S.K., Green S.M., Luo L., Politis C., Durczewski K., Ausloos M. (1989). *Mod. Phy. Lett. B* 3 241.
Leea A.T., Richards L.P., Nam S.W., Cabrera B., Irwin K.D. (1996). *Appl. Phys. Lett.* 69 12
Lopez A.J., Maza J., Yadava Y.P., Vidal F., Garcia-Alvarado F., Morán E., Senaris-Rodriguez M.A. (1991). *Supercond. Sci. Technol*. 4 S292
Maeda A., Yabe T., Takebayashi S., Hase M., Uchinokura K. (1990). *Phys. Rev. B* 41 4112
Mitra N., Trefny J., Yarar B., Pine G., Sheng Z.Z., Hermann A.M. (1988). *Phys. Rev. B* 38 7064.
Majewski P. (2000). J. *Mater. Res.* 15 4.
Maqsood A., Amin N., Maqsood M., Shabbir G., Mahmood A., Gustafsson S.E. (1994). *Int. J. Energy Res.* 18 777.
Maqsood M., Arshad M., Zafarullah M., Maqsood A. (1996). *J. Supercond. Sci. Technol.* 9 321.
Maqsood A., Khaliq M., Maqsood M. 1992). *J. Mat. Sci.* 27 5330
Maqsood A., Rehman M.A., Gumen V., Haq A. (2000). *J. Phys D: Appl. Phys.* 33 2057.
Microsoft Encarta Encyclopedia. (2003). Microsoft Corporation, USA
Mori N., Wilson J.A., Ozaki H. (1992). *Phys. Rev. B* 45 10633.
Mori K., Sasakawa M., Igarashi T., Isikawa Y., Sato K., Noto K., Muto Y. (1989). *Physica C* 162 512.
Muller K.H. (1989). *Physica C* 159 717.
Naqvi S.M.M.R., Rizvi S.D.H., Rizvi S., Raza S.M. (1997). Proc. *5th International Symposium on Advanced Materials*, Islamabad
Okazaki N., Hasegawa T., Kishio K., Kitazawa K., Kishi A., Ikeda Y., Takano M., Oda K., Kitaguchi H., Takada J., Miura Y. (1990). *Phys. Rev. B* 41 4296
Peacor S.D. , Uher C. (1989). *Phys. Rev. B* 39 11559
Pekala M., Tampieri A., Celotti G., Houssa M., Ausloos M. (1996). *Supercond. Sci. Technol.* 9 644.
Pop A.V., Deltour R., Harabor A., Ciurchea D., Ilonca Gh., Pop V., Todica M. (1997) . Supercond. Sci. Technol. 10 943.
Rehman M.A., Maqsood A. (2002). *J. Phys D: Appl. Phys* 35 2040.
Rehman M.A., Maqsood A. (2003). *Int. J. of Thermophys.* 24 867.
Rehman M.A., Maqsood M., Ahmad N., Maqsood A., Haq A. (1998). *J. Mat. Sci.* 33 1789.
Remschnig K., Tarascon J.M., Miceli P.F., Hull G.W. (1991). *Phys. Rev. B* 43 5481
Richards P.L. (1994). *J. Appl. Phys.* 76 1.
Seeber B. (1998). *Handbook of Applied Superconductivity* vol. 1, Institute of Physics Publishing, Bristol and Philadelphia
Tewordt L., Fay D., Wolkhausen Th. (1988). *Solid State Commun*. 67 301.

Uher C., Kaiser A.B. (1987). *Phys. Rev. B* 36 5680.
vom Hedt B., Lisseck W., Westerholt K., Bach H. (1994). *Phys. Rev. B* 49 9898.

IntechOpen

IntechOpen

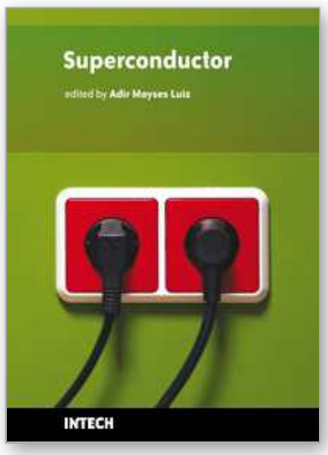

Superconductor

Edited by Doctor Adir Moyses Luiz

ISBN 978-953-307-107-7
Hard cover, 344 pages
Publisher Sciyo
Published online 18, August, 2010
Published in print edition August, 2010

This book contains a collection of works intended to study theoretical and experimental aspects of superconductivity. Here you will find interesting reports on low-Tc superconductors (materials with Tc< 30 K), as well as a great number of researches on high-Tc superconductors (materials with Tc> 30 K). Certainly this book will be useful to encourage further experimental and theoretical researches in superconducting materials.

How to reference

In order to correctly reference this scholarly work, feel free to copy and paste the following:

Anis-ur-Rehman Muhammad and Asghari Maqsood (2010). Synthesis and Thermophysical Characterization of Bismuth Based High-Tc Superconductors, Superconductor, Doctor Adir Moyses Luiz (Ed.), ISBN: 978-953-307-107-7, InTech, Available from: http://www.intechopen.com/books/superconductor/synthesis-and-thermophysical-characterization-of-bismuth-based-high-tc-superconductors

INTECH
open science | open minds

InTech Europe
University Campus STeP Ri
Slavka Krautzeka 83/A
51000 Rijeka, Croatia
Phone: +385 (51) 770 447
Fax: +385 (51) 686 166
www.intechopen.com

InTech China
Unit 405, Office Block, Hotel Equatorial Shanghai
No.65, Yan An Road (West), Shanghai, 200040, China
中国上海市延安西路65号上海国际贵都大饭店办公楼405单元
Phone: +86-21-62489820
Fax: +86-21-62489821

© 2010 The Author(s). Licensee IntechOpen. This chapter is distributed under the terms of the Creative Commons Attribution-NonCommercial-ShareAlike-3.0 License, which permits use, distribution and reproduction for non-commercial purposes, provided the original is properly cited and derivative works building on this content are distributed under the same license.

IntechOpen

IntechOpen